Defense Technical Information Center Compilation Part Notice

ADP011021

TITLE: Planar Synthesis of Anisotropic Nanoparticles

DISTRIBUTION: Approved for public release, distribution unlimited

This paper is part of the following report:

TITLE: Materials Research Society Symposium Proceedings Volume 635.
Anisotropic Nanoparticles - Synthesis, Characterization and Applications

To order the complete compilation report, use: ADA395000

The component part is provided here to allow users access to individually authored sections
of proceedings, annals, symposia, etc. However, the component should be considered within
the context of the overall compilation report and not as a stand-alone technical report.

The following component part numbers comprise the compilation report:
ADP011010 thru ADP011040

Planar Synthesis of Anisotropic Nanoparticles

Gennady B. Khomutov, Radmir V. Gaynutdinov[1], Sergey P. Gubin[2], Alexander Yu. Obydenov, Eugene S. Soldatov, Alla L. Tolstikhina[1], Artem S. Trifonov
Faculty of Physics, Moscow State University, Moscow 119899, Russia, GBK@phys.msu.su
[1]Institute of Crystallography RAS, Moscow 119899, Russia
[2]Institute of General and Inorganic Chemistry RAS, Moscow 119899, Russia

ABSTRACT

A novel method of two-dimensional (2-D) synthesis of anisotropic nanoparticles have been developed in which nanoparticle growth is an example of 2-D process where true 2-D diffusion of precursor molecules and active intermediates, metal atoms and its complexes, nucleus and growing nanoparticles, surfactants and additives occurs only in the plain of a monolayer at the gas/liquid interface. Nanoparticles were generated via ultraviolet decomposition of a volatile insoluble metal-organic precursor compound (iron pentacarbonyl) and by chemical reduction of palladium from $Pd_3(CH_3COO)_6$ molecules in a mixed Langmuir monolayer with stearic acid, arachidic acid or octadecyl amine on the aqueous subphase surface. The properties of such surfactants to form Langmuir monolayer and to prevent aggregation of nanoparticles were here combined successfully. Atomic force microscopy, scanning tunneling microscopy and transmission electron microscopy techniques were used to study morphology of deposited nanoparticulate monolayers. The size and shape of nanoparticles were dependent substantially on the monolayer composition and state during the synthesis process. We demonstrate that planar synthesis in a monolayer at the gas/liquid interface allows to produce anisotropic extremely flat nanoparticles with very high surface to volume ratio and unique morphologies such as iron-containing magnetic nano-rings.

INTRODUCTION

Synthesis of nanosize metal-containing particles (metallic, oxidic and semiconductor) has recently drawn great attention because of their unique physicochemical properties and potentially wide applications in diverse devices and processes exploiting nanophase and nanostructured materials [1-3]. Anisotropic nanoparticles are of particular interest for basic and applied studies due to the anisotropy of size-dependent properties and substantial surface effects which can result in much more rich and enhanced physical and chemical properties compared to the conventional isotropic spherical particles. Therefore, development of novel methods for effective shape and size control of nanoparticles is of principal importance for nanoparticles research. The method of nanoparticles synthesis often influences the properties of the product, particularly the shape, size, crystal morphology and degree of crystallinity [4-11]. A novel approach to the synthesis of anisotropic nanoparticles was introduced recently in which nanoparticles were fabricated in a mixed Langmuir monolayer at the gas/liquid interface [12]. In the present study, nanoparticles were generated by the ultraviolet (UV) decomposition of $Fe(CO)_5$, and by chemical reduction of palladium from $Pd_3(CH_3COO)_6$ in mixed monolayers with stearic acid, arachidic acid or octadecyl amine onto the aqueous subphase surface. Atomic force microscopy (AFM), scanning tunneling microscopy (STM) and transmission electron microscopy (TEM) were used to image grown nanoparticles.

EXPERIMENTAL DETAILS

Stearic acid (SA), arachidic acid (AA) and octadecyl amine (ODA) were obtained

from Aldrich/Sigma. Iron pentacarbonyl was obtained from Alfa Inorganic. $Pd_3(CH_3COO)_6$ was obtained and purified by Prof. S.P. Gubin using known procedures. A MilliQ water purification system was used to produce clean water with an average resistivity of 18 MΩ-cm. Iron-containing nanoparticles were fabricated by the UV decomposition (UV irradiation from 300 mW conventional UV source, $\lambda \cong 300$ nm) of iron pentacarbonyl, a volatile water-insoluble metal-organic compound, in a mixed Langmuir monolayer formed by spreading an appropriate amount of the chloroform solution of $Fe(CO)_5$ with SA on the surface of purified water (pH=5.6). To synthesize Pd nanoparticles, the mixed solution of $Pd_3(CH_3COO)_6$ (water-insoluble precursor) with AA or ODA in chlorophorm was spread onto the surface of aqueous phase containing $NaBH_4$ as reducing agent. Nanoparticles then were synthesized in the mixed Langmuir monolayer formed after fast solvent evaporation on the surface of aqueous phase (incubation time 30 min, 21 °C). Langmuir monolayer formation, surface pressure (π) - monolayer area isotherm measurements and nanoparticulate monolayer transfer to solid substrates were carried out on a full automatic conventional Teflon trough as described elsewhere [12, 13]. Mica (for AFM study) and graphite (for STM study) substrates were freshly cleaved immediately before use. Samples for TEM measurements were prepared by direct collection of the nanoparticulate monolayer material from the aqueous subphase surface onto the Formvar film supported by the copper grid (diameter = 3 mm), then samples were dried and subjected to TEM analyses with the use of Jeol JEM-100B microscope. AFM measurements were performed with the use of Solver P47-SPM-MDT scanning probe microscope (NT MDT Ltd., Moscow, Russia) in a tapping mode. Images were measured in air at ambient temperature (21 °C) and were stable and reproducible. STM topographic images were obtained by recording the tip height at a constant tunnel current in a modified Nanoscop I microscope (Digital Instruments, U.S.A.) at ambient temperature. Tunnel current I = 0.3 nA, and a bias voltage V_{bias} = 200 mV.

RESULTS AND DISCUSSION

Typical STM image of the ultraflat iron-containing nanoparticle photochemically generated in a mixed iron pentacarbonyl/SA monolayer is shown in figure 1. In a sence, such system where 2-D arranged precursor molecules are photochemically decomposed with initiation of 2-D reactions of nanoparticles growth represents an ultimately thin photosensitive
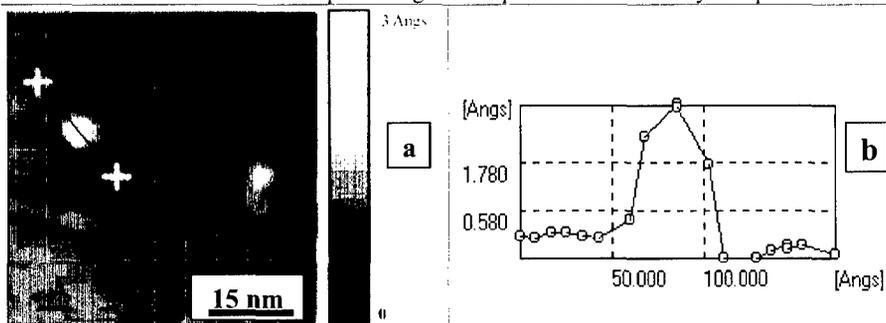

Figure 1. a): *STM topographic image (top view) of individual iron-containing nanoparticle synthesized in a mixed Langmuir monolayer and deposited by horizontal lifting method onto the surface of high oriented pyrolytic graphite substrate. Reaction conditions: initial Fe(CO)$_5$/SA ratio in monolayer was 10:1, UV exposure time 3 min, T = 294 K, subphase pH = 5.6, uncompressed monolayer (π = 0). The white crosses and black line mark the position of cross-section. b)*: *Cross-section profile of the nanoparticle shown on figure 1a).*

structure. Figure 2 shows corresponding AFM images of the nanoparticulate monolayer deposited onto the surface of mica substrate. Figure 2b) demonstrates AFM phase contrast regime image corresponding to the image 2a) revealing the difference in material of circular objects and surrounding SA matrix, thus indicating grown nanoparticles. Figure 1c) shows the typical height cross section profile of the image 1a) and indicates an overall film roughness of ~ 4 nm with clearly observable nanoparticles of the volkano-like morphology with obvious cavity in the central part. Nanoparticles are very flat (height about 1 nm) with very high surface-to-volume ratio (diameter/height ratio ~ 100). Nanoparticles grown in the compressed mixed monolayer (figure 2d) are characterized by significantly larger diameter (~ 200 nm and more), noncircular shape, but also by extremely small height (~ 2 nm). Some nanoparticles possessed ledges of ~ 5 nm height and formed aligned aggregates clearly seen in figure 2d). Such differences in morphologies of nanoparticles indicate that kinetic factors (anisotropic 2-D diffusion and surface concentration of reagents and active intermediates) and complex
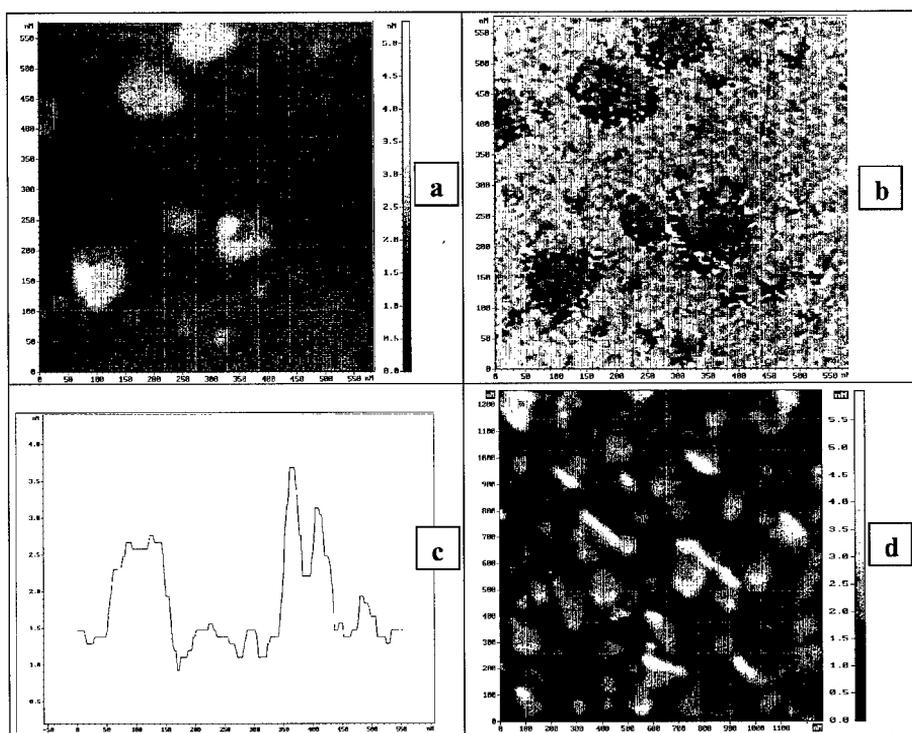

Figure 2. *AFM tapping mode topographic images of iron-containig nanoparticles synthesized in the mixed floating monolayer (initial $Fe(CO)_5$/SA ratio was 10:1, UV exposure time 4 min, T = 294 K, subphase pH = 5.6) and deposited onto the mica substrate at π = 25 mN/m using vertical substrate lifting method. **a**): nanoparticles were synthesized at π = 0, top view image, 580×580 nm^2 scan area, the black-to-white color height scale is 0 -5 nm. **b**): AFM phase contrast mode top view image corresponding to the image 2a). **c**): Typical height cross-section profile of image 2a). **d**): top view image of nanoparticles synthesized in a compressed monolayer (surface pressure during the synthesis of nanoparticles was $\pi \cong 2$ mN/m) 1.25×1.25 μm^2 scan area, the black-to-white color height scale is 0 – 6 nm.*

structure of mixed compressed monolayer can play important role in the determination of nanoparticle morphology in the 2-D synthesis method.

Figure 3 illustrates the possibilities of 2-D synthesis approach to control the shape of noble metal, in particularly, Pd nanoparticles. In this embodiment the reduction of palladium in a mixed precursor plus surfactant monolayer floating on the surface of the aqueous subphase with sodium borohydride can be considered as an ultimate version of a two-phase reducing system in which precursor phase represents a monomolecular structure. It follows from figure 3 that the morphology of grown Pd nanoparticles is dependent on the presence of surfactant in the monolayer and on the nature of surfactant used. The homogeneous flat morphology of nanoparticles is clearly illustrated by figure 3c) where height histogram of the image 3a) is presented with two broad peaks corresponding to the most frequently present structure heights with main height difference about 2.4 nm demonstrating the terrace structure of the particulate monolayer with probable main Pd nanoparticle height about 2.4 nm.

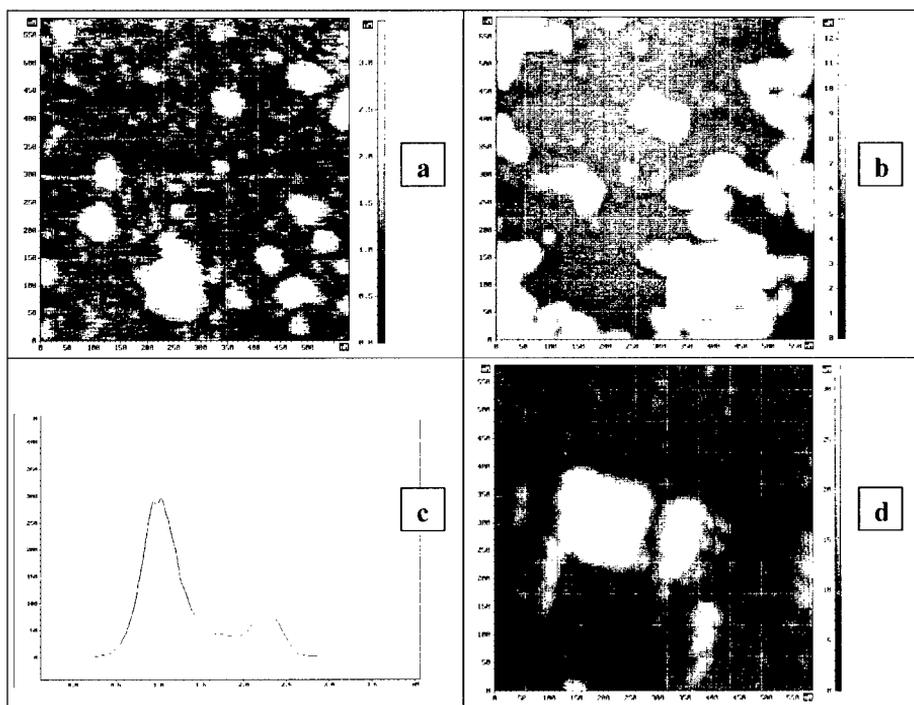Figure 4 shows TEM micrographs obtained from corresponding nanoparticulate

Figure 3. *AFM tapping mode topographic images of Pd nanoparticles synthesized in a monolayer at the gas/NaBH₄ solution (5×10⁻³ M) interface at π = 0, T = 294 K, and deposited onto the mica substrate.* **a)**: *top view image, 580×580 nm² scan area, the black-to-white color height scale is 0 - 3 nm, spreading solution of Pd₃(CH₃COO)₆/ODA with 1:1 ratio in chlorophorm (10⁻⁴ M ODA) was used.* **b)**: *top view image, 580×580 nm² scan area, the black-to-white color height scale is 0 - 12.5 nm, spreading solution of Pd₃(CH₃COO)₆/AA with 1:1 ratio in chlorophorm (10⁻⁴ M AA) was used.* **c)**: *height histogram of the image 3a).* **d)**: *top view image, 580×580 nm² scan area, the black-to-white color height scale is 0 - 35 nm, spreading solution of Pd₃(CH₃COO)₆ in chlorophorm (10⁻⁴ M) without surfactant was used.*

samples giving evidence for amorphous character of iron-containing nanoparticles and polycrystalline metallic Pd nanoparticles with morphology being in good agreement with STM and AFM data. Earlier we have observed ferromagnetic resonance and superparamagnetic signals in the material with iron-containing nanoparticles, indicating magnetic moments of the grown particles [14]. It was also found that the size and shape anisotropy of iron-containing nanoparticles grown under applied external fields were strongly dependent on the applied field orientation relatively to the monolayer surface [14, 15].
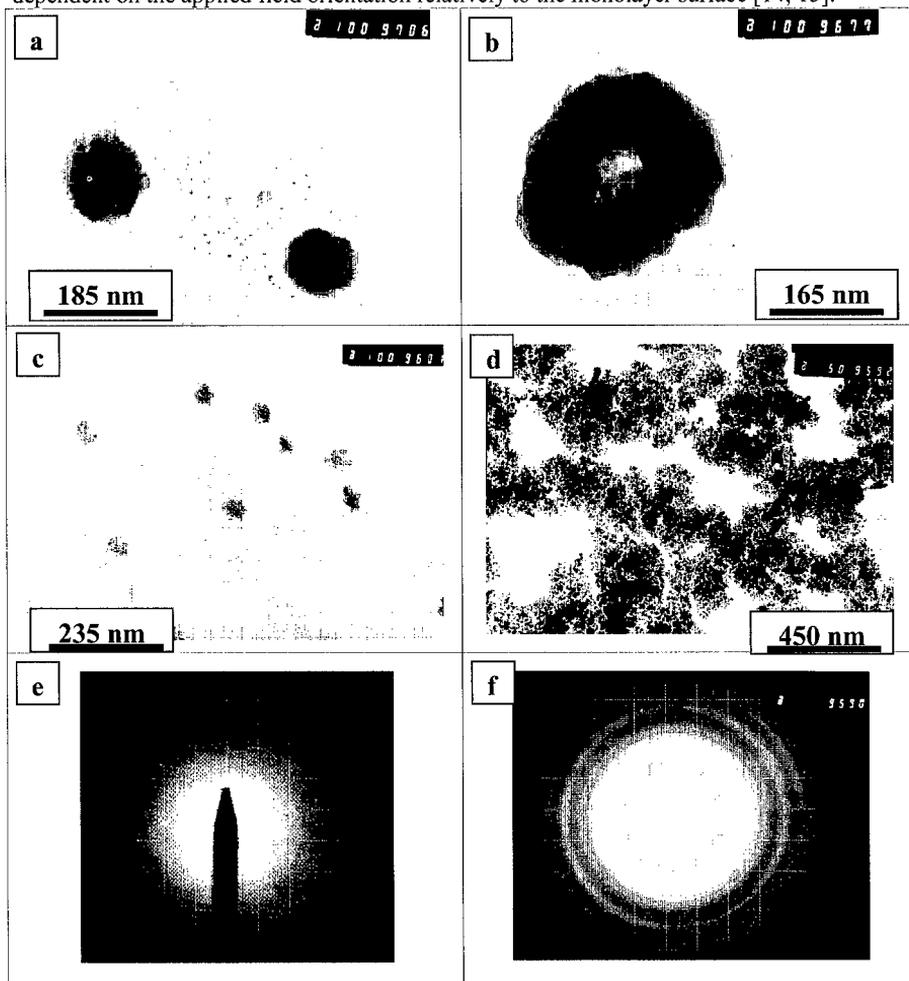

Figure 4. *Transmission electron micrographs showing nanoparticles grown in Langmuir monolayer and deposited onto the copper grid with Formvar coating. Conditions for nanoparticle synthesis: for images a) and b) the same as in figure 2a), for image c) the same as in figure 3a), for image d) the same as in figure 3b). Image e) – selected area electron diffractogramm obtained from amorphous iron-containing nanoparticles (images 4a) and 4b)). Image f) – selected area electron diffraction pattern obtained from nanoparticles shown on images 4c) and 4d) indicating polycrystalline Pd.*

CONCLUSIONS

A novel approach to the synthesis of anisotropic nanoparticles is developed in which nanoparticles are fabricated via decomposition of an insoluble metal-organic precursor compound in a mixed surfactant monolayer at the gas/liquid interface accompanied by 2-D reactions of nanoparticles growth. It is demonstrated that such 2-D synthesis method allows to produce anisotropic extremely flat inorganic nanoparticles including noble metal nanoparticles with very high surface to volume ratio and unique morphologies such as iron-containing magnetic nanoparticles with characteristic nano-ring shape. Controlling the morphology of nanoparticles via planar synthesis in a monolayer at the gas/liquid interface and/or under applied external fields opens new possibilities for regulation of the nanoparticles growth processes to obtain anisotropic inorganic nanostructures with different predetermined morphologies what could prove to be a promising approach for nanotechnology, nanophase engineering and creation of new nanostructured bulk materials and ultrathin films (down to monolayer thickness) with advanced, in particularly, highly anisotropic physical and chemical properties perspective for applications.

ACKNOWLEDGMENTS

REFERENCES

1. A.P. Alivisatos, *Science*, **271**, 933 (1996).
2. C.P. Collier, R.J. Saykally, J.J. Shiang, S.E. Henrichs and J.R. Heath, *Science*, **277**, 1978 (1997).
3. I. Pastoriza-Santos, D.S. Koktysh, A.A. Mamedov, M. Giersig, N.A. Kotov and L.M. Liz-Marzan, *Langmuir,* **16**, 2731 (2000).
4. *Nanoparticles in solids and solutions*, ed. J.H. Fendler and I. Dekany (Kluwer Academic Publishers, 1996).
5. T.S. Ahmadi, Z.L. Wang, T.C. Green, A. Henglein and M.A. El-Sayed, *Science*, **272**, 1924 (1996).
6. J. Zhu, S. Liu, O. Palchik, Yu. Koltypin and A. Gedanken, *Langmuir,* **16**, 6396 (2000).
7. C.K. Preston and M. Moskovits, *J. Phys. Chem*, **97**, 8495 (1993).
8. Y.Y. Yu, S.S. Chang, C.L. Lee and C.R.C. Wang, *J. Phys. Chem. B*, **101**, 6661 (1997).
9. S. Ravaine, G.E. Fanucci, C.T. Seip, J.H. Adair, D.R. Talham, *Langmuir*, **14**, 708 (1998).
10. E.S. Smotkin, C. Lee, A.J. Bard, A. Campion, M.A. Fox, T.E. Mallouk, S.E. Webber and J.M. White, *Chem. Phys. Lett.*, **152**, 265 (1988).
11. A.V. Nabok, A.K. Ray, A.K. Hassan, J.M. Titchmarsh, F. Davis, T. Richardson, A. Starovoitov and S. Bayliss, *Mat. Sci. Eng. C*, **8-9**, 171 (1999).
12. G.B. Khomutov, A.Yu. Obydenov, S.A. Yakovenko, E.S. Soldatov, A.S. Trifonov, V.V. Khanin, S.P. Gubin, *Mat. Sci. Eng. C*, **8-9**, 309 (1999).
13. G.B. Khomutov, E.S. Soldatov, S.P. Gubin, S.A. Yakovenko, A.S. Trifonov, A.Yu. Obydenov, V.V. Khanin, *Thin Solid Films*, **327-329**, 550 (1998).
14. G.B. Khomutov, S.P. Gubin, Yu.A. Koksharov, V.V. Khanin, A.Yu. Obidenov, E.S. Soldatov, A.S. Trifonov, *Mat. Res. Soc. Symp. Proc.*, **577**, 427 (1999).
15. S.P. Gubin, A.Yu. Obydenov, E.S. Soldatov, A.S. Trifonov, V.V. Khanin and G.B. Khomutov, *PCT International Patent* WO 00/15545, Application RU99/00091, Filed 30.03.1999., Published 23.03.2000, Priority date 11.09.98.